Liquid Crystals

Effects of benzoyl group substituents on the mesomorphic properties of 5-alkoxy-2-benzoylaminotropones

Akira Mori Corresponding author[a]; Katsuyuki Uno[a]; Kanji Kubo[a]; Nobuo Kato[a]; Hitoshi Takeshita[a]; Ken Hirayama[b]; Seiji Ujiie[c]

[a] Institute for Materials Chemistry and Engineering, 86 Kyushu University, Kasuga-koen, Kasuga, Fukuoka 816-8580, Japan [b] Graduate School of Engineering Sciences, 39 Kyushu University, Kasuga-koen, Kasuga, Fukuoka 816-8580, Japan [c] Department of Material Science, Interdisciplinary Faculty of Science and Engineering, Shimane University, Matsue 690-8504, Japan

PLEASE SCROLL DOWN FOR ARTICLE

Taylor & Francis
Taylor & Francis Group

Effects of benzoyl group substituents on the mesomorphic properties of 5-alkoxy-2-benzoylaminotropones

AKIRA MORI*, KATSUYUKI UNO, KANJI KUBO, NOBUO KATO, HITOSHI TAKESHITA

Institute for Materials Chemistry and Engineering, 86 Kyushu University, Kasuga-koen, Kasuga, Fukuoka 816-8580, Japan

KEN HIRAYAMA

Graduate School of Engineering Sciences, 39 Kyushu University, Kasuga-koen, Kasuga, Fukuoka 816-8580, Japan

and SEIJI UJIIE

Department of Material Science, Interdisciplinary Faculty of Science and Engineering, Shimane University, Matsue 690-8504, Japan

Three types of 5-alkoxy-2-benzoylaminotropones, containing an electron-donating group and seven types of derivatives with electron-withdrawing groups on the benzoyl group, were prepared in order to study the thermal ranges of the mesophases exhibited. The troponoid amides had higher transition temperatures than the corresponding troponoid esters and benzenoid amides. From the ^{1}H NMR spectroscopic measurements and X-ray crystallographic analysis of 5-butoxy-2-(4-methoxybenzoylamino)tropone, it was observed that the benzoyl carbonyl group faced to the H-3 of the tropone ring to form an intramolecular hydrogen bond between the tropone carbonyl and the amide NH groups. The intramolecular hydrogen bonding of the troponoid amides made the molecules flat, inducing strong π–π intermolecular interactions between head-to-tail dimers and so reduced the possibility of intermolecular hydrogen bonding between the NH group and the carbonyl group of neighbouring molecules so decreasing melting points. Electron-donating groups enhanced the appearance of nematic phases while electron-withdrawing groups promoted smectic A phases.
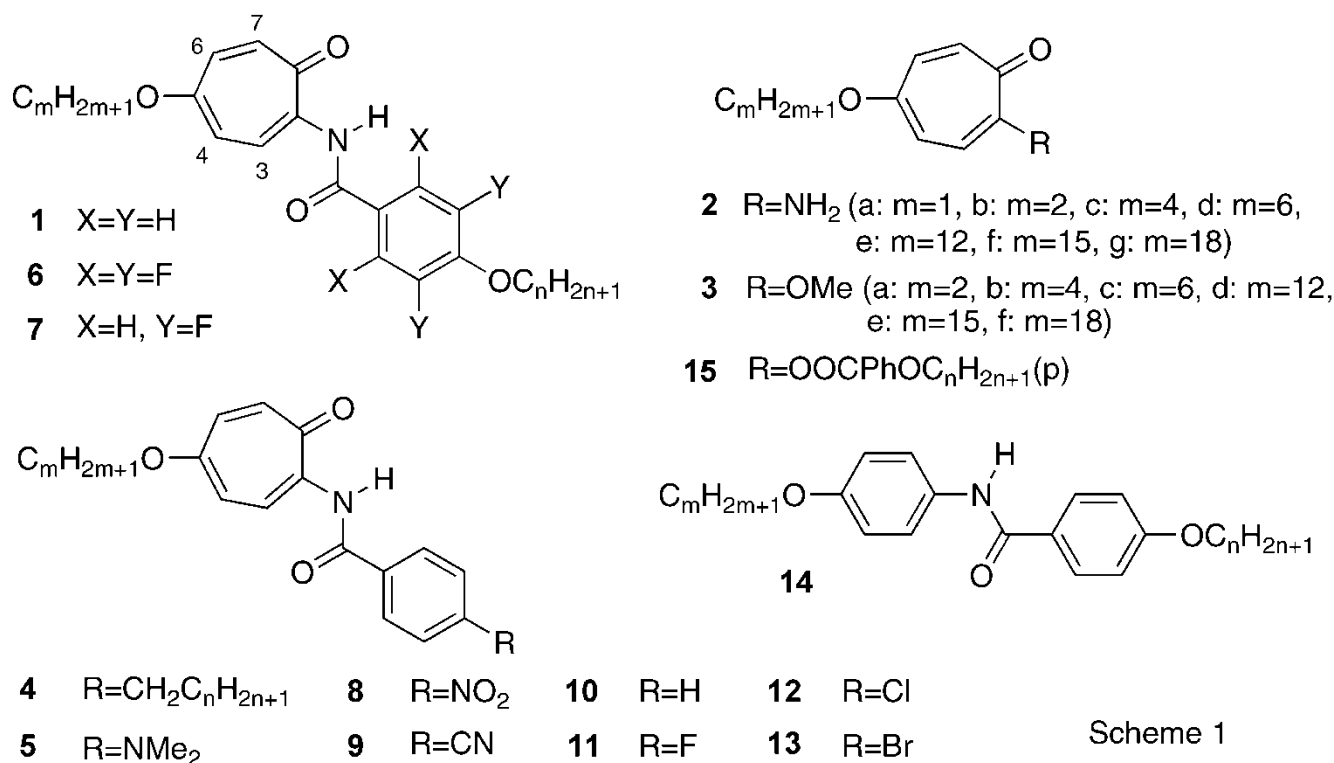
1. Introduction

Intermolecular interactions such as π–π interactions, hydrogen bonding interactions, and dipole–dipole interactions are important factors in the induction of mesophases [1]. We are currently using troponoid cores, a seven-membered ring with a carbonyl group, because they have a large dipole moment [2] to induce layered structures through head-to-tail arrangements [3], and the carbonyl group is able to act as an acceptor of both inter- [4] and intra-molecular hydrogen bonding [3, 5, 6]. Furthermore, the carbonyl group acts as an acceptor fragment of an acyl group in the sigmatropic rearrangement when a molecule has an acyl group at the C-2 position of a tropone ring [7].

Recently, we prepared 5-alkoxy- [6] and 5-cyano-2-benzoylaminotropones [3] and observed that an

amide-connecting group in the C-2 position raised the clearing points when compared with those of the corresponding ester derivatives although it is known that an amide group also increases melting points obscuring liquid crystalline behaviour [8]. In troponoid amide derivatives, however, the amide group made the molecule flat through an intramolecular hydrogen bond between the tropone carbonyl and the NH group. The intramolecular hydrogen bonding reduced the chances of intermolecular hydrogen bonding of the NH group, so decreasing melting points. Hence, the troponoid amides have higher transition temperatures than the troponoid esters [2, 5, 9]. Additionally, we have pointed out that a π–π interaction between neighbouring tropone rings, and a CH–π interaction [10, 11] between the alkoxy side chain on the tropone ring and the benzene ring of neighbouring molecules, contributed to the appearance of mesomorphic properties for

*Author for correspondence; e-mail: mori-a@cm.kyushu-u.ac.jp

1 X=Y=H

6 X=Y=F

7 X=H, Y=F

2 R=NH$_2$ (a: m=1, b: m=2, c: m=4, d: m=6, e: m=12, f: m=15, g: m=18)

3 R=OMe (a: m=2, b: m=4, c: m=6, d: m=12, e: m=15, f: m=18)

15 R=OOCPhOC$_n$H$_{2n+1}$(p)

14

4 R=CH$_2$C$_n$H$_{2n+1}$ **8** R=NO$_2$ **10** R=H   **12** R=Cl

5 R=NMe$_2$ **9** R=CN   **11** R=F   **13** R=Br

Scheme 1

Scheme 1.

5-alkoxy-2-(4-alkoxybenzoylamino)tropones (**1**) [6]. In this paper, we report substituent effects of the benzoyl group on the mesomorphic properties of 5-alkoxy-2-benzoylaminotropones, for which electron-donating groups enhanced nematic (N) behaviour, whereas electron-withdrawing groups promoted smectic A (SmA) phases (see scheme 1).

2. Synthesis

Compounds **1** were prepared from benzoylation of 5-alkoxy-2-aminotropones (**2**), which were obtained from reactions of 5-alkoxy-2-methoxytropones (**3**) with aqueous ammonia in methanol in a sealed tube at 100°C for 12 h. The structure of compounds **1** was determined from the spectral data. In the ^{1}H NMR spectrum of 5-butoxy-2-(4-methoxybenzoylamino)tropone (**1h**), the H-3 of the tropone ring and the amide proton appeared at δ 9.09 (1H, d, $J = 11.0$ Hz) and 9.90 (1H, br s), respectively. Since the H-3 and NH$_2$ protons of 2-amino-5-butoxytropone (**2c**) were observed at δ 6.84 (1H, d, $J = 11.0$ Hz) and 5.53 (2H, br s), respectively, the amide carbonyl group of **1h** was directed outwards to form an intramolecular hydrogen bond between the tropone carbonyl and the NH group and shifted the H-3 proton to lower magnetic fields. Similarly,
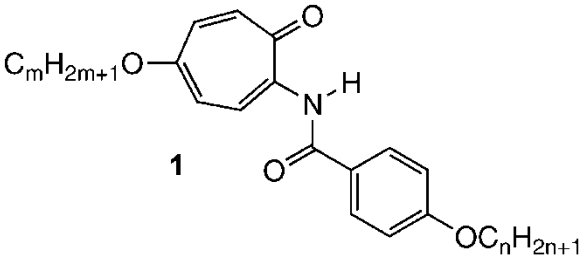
compounds **4–13** were prepared from benzoylation of **2** with the corresponding benzoyl chlorides.

3. Results and discussion

3.1. *Mesomorphic properties of derivatives containing an electron-donating group*

The transition temperatures were determined using differential scanning calorimetry (DSC) and the mesomorphic phases were observed using a polarizing microscope equipped with a hot stage. The transition temperatures of compounds **1** are summarized in table 1†. Compounds **1** show N phases when one of the alkoxy groups is short and N and smectic C (SmC) phases when the two alkoxy groups become long. The mesophase of compound **1h** was assigned as an N phase from the appearance of schlieren texture and by X-ray diffraction (XRD) analysis, in which no reflection was observed in the small angle region. The mesophase of compound **1t** was determined to be a SmC phase

†All transition temperatures were obtained by microscopic observations. The data of **1a–c** and **1e–h** are not the same as data in reference [6] because they were obtained by DSC measurements. Thermal behaviours of **1e** and **1f** should be revised.

Table 1. Transition temperatures (°C) and yields (%) of compounds **1**.

Compound	*m*	*n*	Yield	Cr		SmC		N		I
1a	1	1	67	●	177					●
1b	1	2	91	●	156			●	(110)[a]	●
1c	1	4	41	●	121			●	(110)	●
1d	1	12	55	●	115			●	(102)	●
1e	2	1	38	●	135			●	(131)	●
1f	2	2	87	●	146			●	(137)	●
1g	2	12	84	●	102			●	109	●
1h	4	1	64	●	105			●	113	●
1i	4	2	41	●	104			●	123	●
1j	4	3	53	●	95			●	115	●
1k	4	4	35	●	98			●	122	●
1l	4	5	45	●	82			●	114	●
1m	4	6	79	●	69			●	117	●
1n	6	1	66	●	101			●	108	●
1o	6	12	88	●	67			●	102	●
1p	12	1	78	●	85			●	103	●
1q	12	2	97	●	80			●	108	●
1r	12	12	86	●	79	●	107	●	112	●
1s	15	1	66	●	78			●	99	●
1t	15	12	97	●	81	●	112			●
1u	18	2	88	●	85			●	103	●
1v	18	12	72	●	90	●	111			●

[a]() Indicates monotropic transition.

from the observation of schlieren and focal-conic fan textures.

The thermal stability of the mesophases depends on the length of the alkoxy side chains. Compound **1a** with two methoxy groups was non-mesomorphic. The N phase of compound **1b** with an ethoxy group on the benzoyl group appeared on cooling at 110°C, and that of compound **1e** with an ethoxy group on the tropone ring at 131°C. The temperature difference between **1b** and **1e** is 21°C. Comparing with the clearing points of **1b** and **1f**, the latter increased by 27°C. On the other hand, the clearing point of **1f** is 6°C higher than that of **1e**. The extension of the alkyl chain on the tropone ring is more effective in enhancing the clearing point than increasing that on the benzoyl group, although the difference between the clearing points **1d** and **1g** is 7°C and between **1p** and **1q** is 5°C.

The X-ray crystallographic analysis of **1h** is shown in figure 1. The core structure is almost coplanar due to

Figure 1. X-ray crystallographic analysis of compound **1h**.

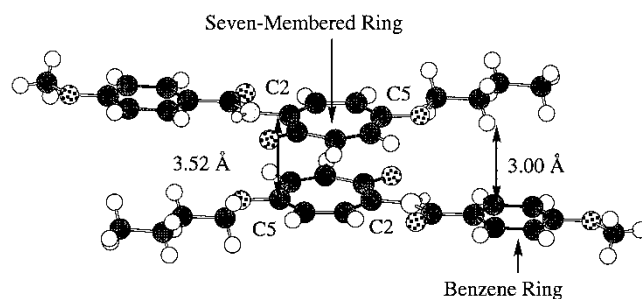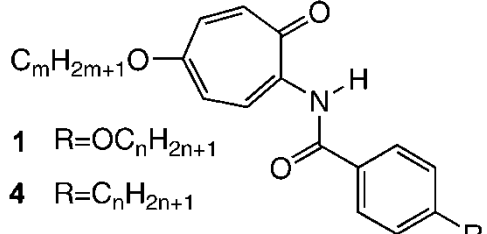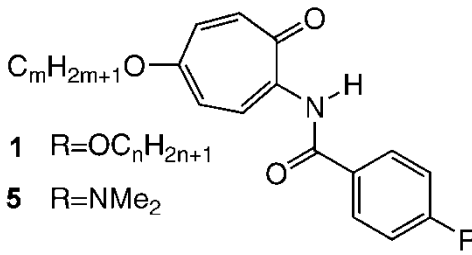intramolecular hydrogen bonding between the tropone carbonyl and the NH group as observed in the ^{1}H NMR spectra. Furthermore, compound **1h** formed a head-to-tail dimer, where the distance between the second methylene hydrogen atom of the butoxy group at the C-5 position and the benzene ring of a neighbouring molecule is 3.00 Å, and the closest distance between two tropone rings is 3.55 Å. The former is close to the value (2.9 Å) of the sum of van der Waals radii (1.7 Å) of a sp^2 carbon atom and a C–H bond length (1.2 Å); the latter is close to the sum (3.4 Å) of that of two sp^2 carbon atoms. The X-ray crystallographic data indicated the presence of intermolecular interactions such as CH–π and π–π interactions in the single crystal state, which suggests that these interactions would play a role also to enhance the thermal stability of the mesophases [6].

Next, the alkoxy group on the benzoyl group was replaced by an alkyl and an *N,N*-dimethylamino (NMe$_2$) group. The transition temperatures of compounds **4** and **5** are summarized in tables 2 and 3. As

Table 2. Transition temperatures (°C) of compounds **4** and **1** and yields (%) of **4**.

1 R=OC$_n$H$_{2n+1}$

4 R=C$_n$H$_{2n+1}$

m	*n*	Yield	Transition temperatures	
2	1	**4a** 72	Cr ● 121 ● I	**1e** Cr ● 135 ● (N ● 131 ●)I
2	2	**4b** 73	Cr ● 117 ● (N ● 105 ●)I	**1f** Cr ● 146 ● (N ● 137 ●)I
4	2	**4c** 74	Cr ● 78 ● N ● 88 ● I	**1i** Cr ● 104 ● N ● 123 ● I
12	2	**4d** 98	Cr ● 68 ● SmA ● 80 ● N ● 89 ● I	**1q** Cr ● 80 ● N ● 108 ● I

Table 3. Transition temperatures (°C) of compounds **5** and **1** and yields (%) of **5**.

1 R=OC$_n$H$_{2n+1}$

5 R=NMe$_2$

m		Yield	R = N(CH₃)₂		R = OCH₃
2	**5a**	47	Cr • 189 • I	**1e**	Cr • 135 • (N • 131 •)I
6	**5b**	56	Cr • 135 • (N • 121 •)I	**1n**	Cr • 101 • N • 108 • I
12	**5c**	58	Cr • 110 • N • 112 • I	**1p**	Cr • 85 • N • 103 • I
15	**5d**	31	Cr • 113 • (N • 107 •)I	**1s**	Cr • 78 • N • 99 • I

seen in table 2, the thermal stability of compounds **4** was reduced compared with that of compounds **1** because an alkyl group is less electron-donating than an alkoxy group. On the other hand, compounds **5** have higher thermal stability than **1** because an NMe$_2$ group is a more electron-donating group than an alkoxy group. This supports the view that the enhancement of the electron density of the benzoyl group is more important in increasing the thermal stability of the mesophase, suggesting the importance of the contribution of the CH–π interaction on the thermal stability.
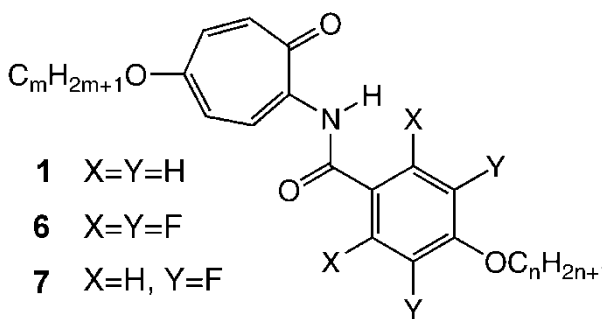
3.2. Mesomorphic properties of fluorinated derivatives

We introduced fluorine atoms on the benzoyl group to reduce the electron density. Tetrafluorinated

X=H, X=F   **16**

X=H, X=F   **17**   Scheme 2
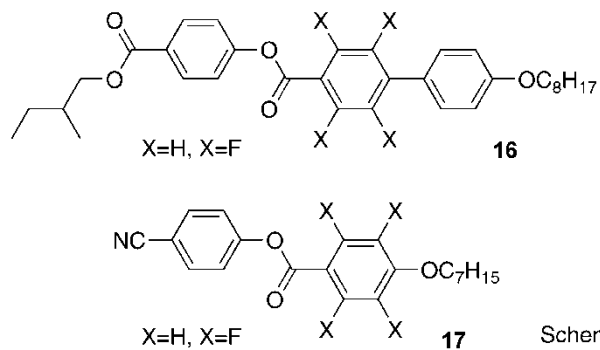
Scheme 2.

compounds **6** were not mesomorphic; the results are summarized in table 4. The introduction of four fluorine atoms increased the melting points so obscuring mesomorphic behaviour. It has been reported that the effect of fluorine atoms on the transition temperatures depends on the core structures. The melting points of the 4-alkoxycarbonylphenyl 2,3,5,6-tetrafluoro-4′-alkoxybiphenylcarboxylates (**16**) were increased and the clearing points decreased [12], whereas for the 4-cyanophenyl 2,3,5,6-tetrafluoro-4-alkoxybenzoates (**17**) the melting points decreased but the mesomorphic behaviour disappeared [13] when compared with the non-fluorinated compounds [14, 15] (see scheme 2). If compound **6b** formed a head-to-tail dimer in a mesophase as observed for compound **1h**, the formation of a tightly packed molecular structure may be sterically less favoured because the core part of **6b** would not be coplanar due to steric repulsion between the two

Table 4. Transition temperatures (°C) of compounds **6**, **7**, and **1** and yields (%) of **6** and **7**.

1 X=Y=H

6 X=Y=F

7 X=H, Y=F

m	n		Yield	X = Y = F		Yield	X = H, Y = F		X = Y = H
1	1	**6a**	33	Cr • 182 • I				**1a**	Cr • 177 • I
4	1	**6b**	31	Cr • 159 • I	**7a**	75	Cr • 112 • I	**1h**	Cr • 105 • N • 113 • I
15	1				**7b**	77	Cr • 86 • (SmA • 79 •)I		
6	12	**6c**	81	Cr • 89 • I	**7c**	48	Cr • 62 • SmA • 88 • I	**1o**	Cr • 67 • N • 102 • I
12	12	**6d**	93	Cr • 88 • I				**1r**	Cr • 79 • SmC • 107 • N • 112 • I
15	12	**6e**	92	Cr • 93 • I	**7d**	37	Cr • 70 • SmA • 93 • I	**1t**	Cr • 81 • SmC • 112 • I
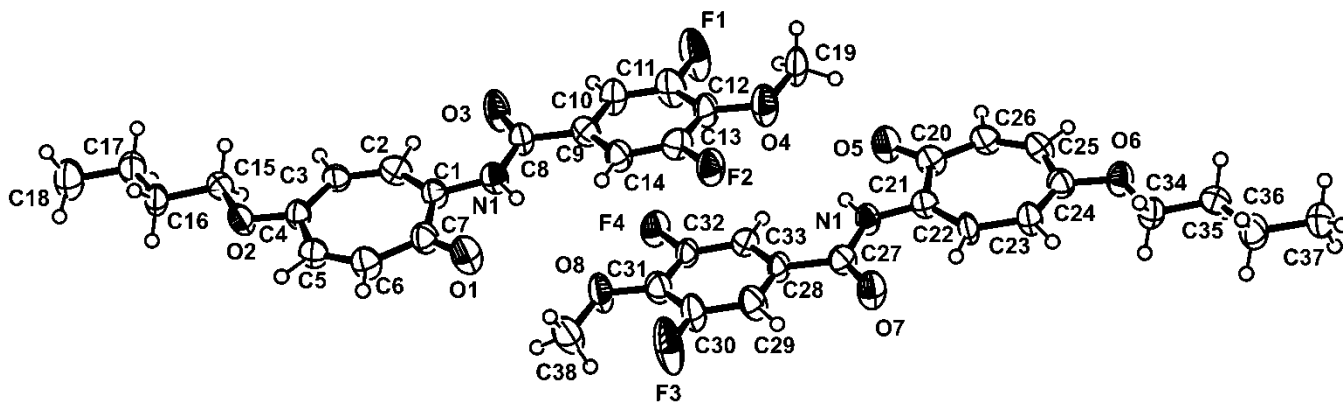
Figure 2.   X-ray crystallographic analysis of compound **7a**.

fluorine atoms at the *ortho*-positions and the benzoyl carbonyl group.

Consequently, we prepared difluorinated molecules **7**, where two fluorine atoms at the *ortho*-positions of the carbonyl group were removed to reduce the steric repulsion. These showed SmA phases with lower clearing points than compounds **1**, as shown in table 4. The X-ray crystallographic analysis of **7a** indicated that the core part of **7a** is nearly flat forming a head-to-tail dimer, where two benzene rings face each other (figure 2). The lower clearing points of **7** are due to the wider molecular width, although the C–F bond length (1.35 Å) is close to the C–H bond length, which favours less the formation of a tight packing structure. Furthermore, the introduction of two fluorine atoms reduced the electron density of the benzoyl group, which would be less favourable for inducing CH–π interaction. These results also support the contribution of the CH–π interaction to the appearance of the mesophases.

3.3. *Mesomorphic properties of derivatives with an electron-withdrawing group*

An electron-withdrawing group was introduced at the C-4 position of the benzoyl group. The transition temperatures are summarized in tables 5 and 6. The compounds with an electron-withdrawing group in table 5 showed SmA phases with higher clearing point than compounds **1** with a methoxy group on the benzoyl group, as summarized in table 3. The XRD study of compound **9d** with a cyano group was measured at 140°C to observe that the layer spacing (*d*) was 35.0 Å. Since the calculated molecular length (*l*) of **9d** is 31.4 Å, they form a SmA phase with the interdigitated head-to-tail arrangement as shown in figure 3. Similarly, compound **8d** with a nitro group showed a similar packing arrangement. Furthermore, XRD study of **12c** with a chlorine atom indicated that the layer spacing was 28.1 Å. Since the calculated molecular length of **12c** is 27.2 Å, using the MM2

Table 5.   Transition temperatures (°C) and yields (%) of compounds **8**, **9**, and **10**.

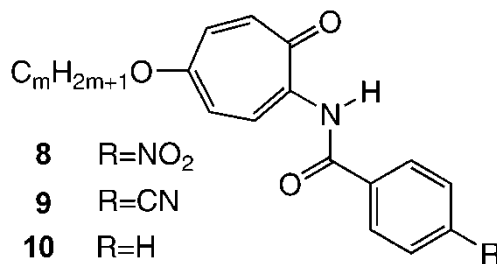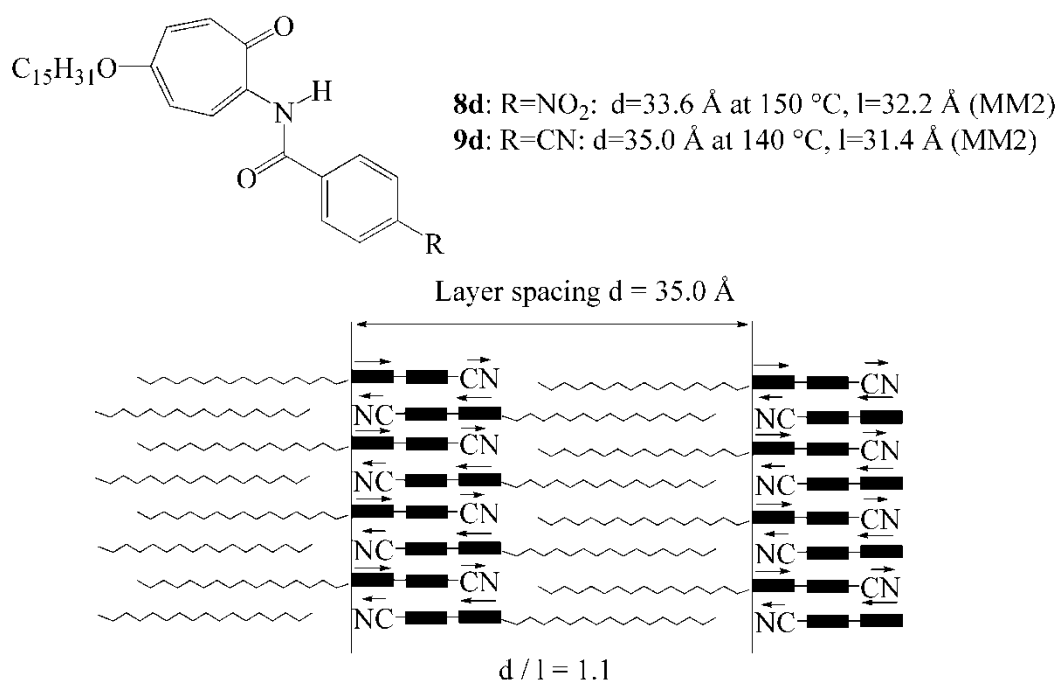| m		Yield	$R = NO_2$		Yield	$R = CN$		Yield	$R = H$
4	**8a**	78	Cr • 156 • I	**9a**	34	Cr • 168 • I			
6	**8b**	71	Cr$_1$ • 128 • Cr$_2$ • 136 • SmA • 152 • I	**9b**	36	Cr • 157 • (N • 133 •)I			
12	**8c**	76	Cr$_1$ • 118 • Cr$_2$ • 125 • SmA • 169 • I	**9c**	58	Cr • 135 • SmA • 148 • I	**10a**	73	Cr • 87 • I
15	**8d**	84	Cr$_1$ • 110 • Cr$_2$ • 126 • SmA • 173 • I	**9d**	57	Cr • 130 • SmA • 151 • I	**10b**	36	Cr • 78 • I

Table 6.   Transition temperatures (°C) and yields (%) of compounds **11**, **12**, and **13**.

11   R=F
12   R=Cl
13   R=Br

m		Yield	R = F		Yield	R = Cl		Yield	R = Br
4	**11a**	26	Cr ● 109 ● I	**12a**	80	Cr ● 128 ● I	**13a**	80	Cr ● 125 ● I
6	**11b**	24	Cr ● 90 ● (N ● 58 ●)I	**12b**	93	Cr ● 108 ● (N ● 95 ●)I	**13b**	76	Cr ● 103 ● (SmA ● 80 ● N ● 95 ●)I
12	**11c**	37	Cr ● 81 ● SmA ● 86 ● I	**12c**	94	Cr ● 88 ● SmA ● 114 ● I	**13c**	91	Cr ● 86 ● SmA ● 114 ● I
15	**11d**	51	Cr ● 76 ● SmA ● 87 ● I	**12d**	82	Cr ● 93 ● SmA ● 113 ● I	**13d**	97	Cr ● 93 ● SmA ● 116 ● I

8d: R=NO$_2$: d=33.6 Å at 150 °C, l=32.2 Å (MM2)
9d: R=CN: d=35.0 Å at 140 °C, l=31.4 Å (MM2)

Layer spacing d = 35.0 Å

d / l = 1.1

Figure 3.   Packing model of compound **9d**.
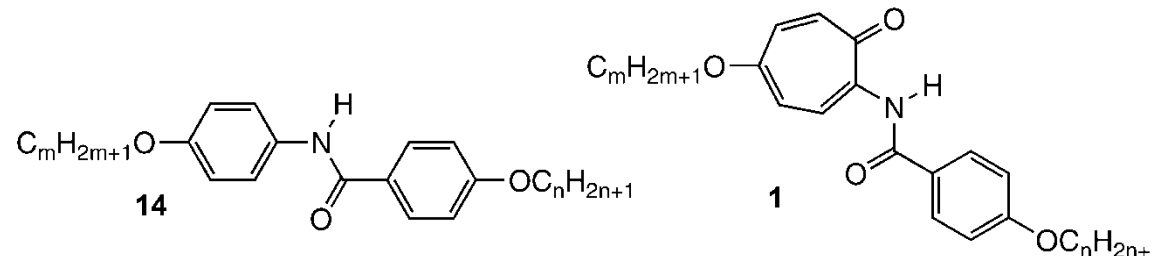
method, compound **12c** formed a monolayer SmA phase.

3.4. *Comparison of mesomorphic properties of troponoids 1 and benzenoids 14*

The transition temperatures of benzenoids **14** are shown in table 7. They have higher melting points than troponoids **1**. Intermolecular hydrogen bonding of **14** increased the melting points to obscure mesomorphic properties. In the case of compounds **1**, the possibility of intermolecular hydrogen bonding at the NH group
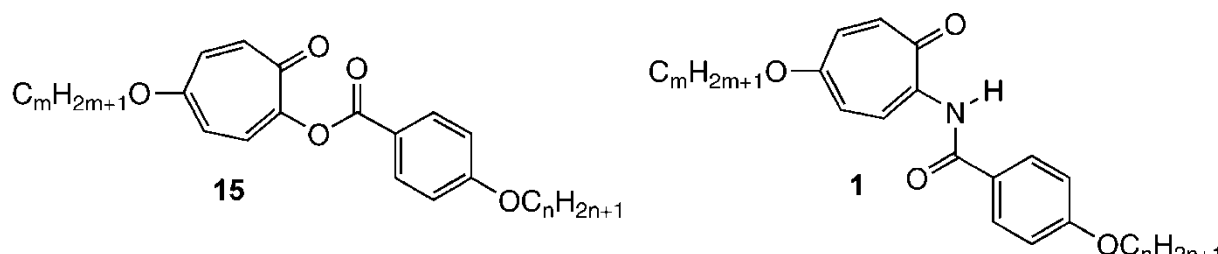
was reduced because of the contribution of the intramolecular hydrogen bond between the tropone carbonyl and the NH group.

3.5. *Comparison of thermal stability of troponoid amides and esters*

Table 8 summarizes the transition temperatures of troponoid esters **15** and amides **1**. Both show N and SmC phases and the amides have higher transition temperatures than the esters. The X-ray crystallographic analysis of compound **1h** indicated that the

Table 7. Transition temperatures (°C) of compounds **14** and **1** and yields (%) of **14**.

m	n		Yield	Transition temperatures		
1	1	14a		Cr • 203 • I[a]	1a	Cr • 177 • I
2	1	14b		Cr • 177 • I[a]	1e	Cr • 135 • (N • 131 •)I
4	6	14c	53	Cr • 153 • I	1m	Cr • 69 • N • 117 • I
6	12	14d	53	Cr • 150 • I[b]	1o	Cr • 67 • N • 102 • I
9	4	14e	55	Cr • 146 • I		

[a]See reference [16, 17].
[b]Microscopy data: Cr • 143.7 • (SmA • 135.0 •)I; see reference [17].

Table 8. Transition temperatures (°C) of compounds **15** and **1**.

m	n		Transition temperatures		
6	1	15a	Cr • 93 • I	1n	Cr • 101 • N • 108 • I
6	4	15b	Cr • 61 • (N • 43 •)I		
6	12	15c	Cr • 58 • (SmC • 54 •)N • 66 • I	1o	Cr • 67 • N • 102 • I
12	1	15d	Cr • 71 • (N • 50 •)I	1p	Cr • 85 • N • 103 • I
12	12	15e	Cr • 64 • SmC • 90 • I	1r	Cr • 79 • SmC • 107 • N • 112 • I
18	12	15f	Cr • 80 • SmC • 66 • I	1v	Cr • 90 • SmC • 111 • I

core part is flat due to an intramolecular hydrogen bond between the tropone carbonyl and the NH group whereas the angle between the seven-membered ring and benzoyl group of 5-(tetradecyloxy)-2-(4-dodecylaminobenzoyloxy)tropone is 76.5° [4] (see table 9). Flat amides have tighter molecular packed structures than twisted esters, so enhancing transition temperatures, especially the clearing points.

4. Conclusion

Liquid crystals consisting of 5-alkoxy-2-benzoylaminotropones were prepared to investigate the benzoyl group substituents on the thermal properties of the mesophases. Electron-donating groups at the *para*-position of the benzoyl group induced N phases, whereas electron-withdrawing groups induced SmA phases. Electron-donating groups on the benzoyl group increased clearing points of N phases. The order of the substituent effect on the thermal stability of the N phase is $NMe_2 > OMe > alkyl$, which parallels the order of electron-donating ability. It has been observed in calamitic liquid crystals that the order of substituent effects on the N–I temperature is $CN > OMe > NO_2 > Cl > Br > NMe_2 > F > H$, where NMe_2 is less favourable than OMe [18]. The electronic considerations overcame the steric ones in the present case. Introduction of fluorine atoms onto the benzoyl group decreased the transition temperatures. This is due to the twisted core structure and the increase of the molecular width of the fluorinated molecules.

Table 9. Crystallographic data for compounds **1h** and **7a**.

Parameter	**1h**	**7a**
Formula	$C_{19}H_{21}NO_4$	$C_{19}H_{19}F_2NO_4$
Formula weight	327.38	363.35
Crystal colour	Pale yellow	Yellow
Crystal size/mm^3	$0.50 \times 0.45 \times 0.30$	$0.50 \times 0.50 \times 0.20$
Crystal system	Monoclinic	Triclinic
Space group	$P2_1/n$	$P\,1$
a/Å	13.196 (3)	10.2122 (13)
b/Å	12.673 (1)	11.527 (2)
c/Å	10.788 (1)	8.1819 (12)
α, β, γ/deg	$\alpha = 107.55$ (2)	$\alpha = 99.0096$ (9)
		$\beta = 112.685$ (7)
		$\gamma = 82.118$ (9)
V/Å^3	1720.3 (5)	874.4 (2)
Z	4	2
D_{calc}/g cm^{-3}	1.26	1.380
μ/mm^{-1}		0.221
No. of reflections	2940	3175
No. of obsd refl. $[I > 2\sigma(I)]$	2098	3123
No. of refined parameters	281	470
Refinement		F^2 (SHELXL97)
$R[F^2 > 2\sigma(F^2)]$	0.049	0.0586
$wR(F^2)$	0.072	0.1747

Next, the compounds with a NO_2 or a CN group formed SmA phases with an interdigitated bilayer structure whereas the compound with a chlorine atom showed monolayer SmA phases. The order of the substituent effect on the thermal stability of the SmA phase is $NO_2 > CN > Br \approx Cl > F$, which parallels the order of electron-withdrawing ability. The NO_2 derivatives had higher clearing points than the CN derivatives. Since the order of the substituent effect is the reverse of that reported [17], it might be possible to form an intermolecular hydrogen bond between the NO_2 and the amide NH groups in the head-to-tail packing model.

When the mesomorphic properties of amides **1** and esters **15** are compared, the former has the higher transition temperatures. This is explained by the planarity of the core structure of amides **1**, which is induced by the intramolecular hydrogen bond between the tropone carbonyl and the NH group. On the other hand, the core structure of ester **15** would twist as observed in an ester derivative, 5-(tetradecyloxy)-2-(4-dodecylaminobenzoyloxy)tropone [4]. It is reasonable to assume that flat cores have stronger intermolecular interactions which enhance the thermal stability.

Compounds **1e** and **1h** have higher clearing points than compounds **1b** and **1c**, in which the lengths of the alkyl chains on the terminal positions is exchanged. The X-ray crystallographic analysis of **1h** indicated tight intermolecular interactions such as CH–π interactions

between the alkoxy group on the tropone ring and the benzene ring of a neighbouring molecule, and π–π interactions between tropone rings, which assisted in promoting higher clearing points.

5. Experimental
5.1. *Characterization*

The elemental analyses were performed at the elemental analysis laboratory of Kyushu University. The NMR spectra were measured on JEOL GSX 270H and Lambda 400 spectrometers in $CDCl_3$; the chemical shifts are expressed in δ units. The mass spectra were measured with a JEOL 01SG-2 spectrometer. The stationary phase for column chromatography was Wakogel C-300 and the eluent was a mixture of ethyl acetate and hexane. The transition temperatures were measured using a differential scanning calorimeter (Seiko DSC 200) and the mesomorphic phase was observed by a polarizing microscope (Olympus BHSP BH-2) equipped with a hot stage (Linkam TH-600RMS). The X-ray diffraction measurements were carried out with a Rigaku Rint 2100 system using Ni-filtered Cu K_α radiation at various temperatures. The measuring temperatures were controlled with a Linkam HFS-91 hot stage. The X-ray crystallographic analyses were carried out with Enraf-Nonius FR 590 and Rigaku RAXIS-RAPID diffractometers.

5.2. *Preparation of 5-ethoxy-2-methoxytropone (3a)*

A chloroform solution of 5-ethoxytropolone [19] (205 mg, 1.23 mmol) was added to an ether solution of diazomethane in an ice bath and the solution stirred overnight. After evaporating the solvent under vacuum, the residue was purified by silica gel chromatography ($CHCl_3$) to give a powder. This was recrystallized (*n*-hexane/AcOEt) to give needle crystals (207 mg, 93%) of **3a** ($m = 2$): m.p. 108°C. ^{1}H NMR δ 1.43 (3H, t, $J = 7.0$ Hz), 3.88 (3H, s), 3.97 (2H, q, $J = 7.0$ Hz), 6.36 (1H, dd, $J = 11.0, 2.6$ Hz), 6.74 (1H, d, $J = 11.0$ Hz), 7.09 (1H, dd, $J = 13.2, 2.6$ Hz), 7.20 (1H, d, $J = 13.2$ Hz). ^{13}C NMR δ 14.4, 55.9, 63.9, 108.2, 113.5, 133.0, 137.0, 158.6, 159.6, 179.3. MS (*m/z*: 70 eV): 180 (52, M$^+$), 151 (26), 123 (100). Analysis: found C 66.31, H 6.66; calcd for $C_{10}H_{12}O_3$ C 66.65, H 6.71%.

5.3. *Preparation of 2-amino-5-methoxytropone (2a)*

A methanol solution of 2,5-dimethoxytropone [19] (113 mg, 0.68 mmol) and 28% aqueous ammonia solution (4 cm^3) was sealed in a glass tube, which was heated at 100°C in an autoclave for 12 h. The reaction mixture was extracted with dichloromethane; the dichloromethane solution was dried over anhydrous $MgSO_4$ and evaporated under vacuum. The residue was

purified by silica gel chromatography (*n*-hexane/AcOEt, 1/1) to give a powder. Recrystallization (*n*-hexane/AcOEt) of the powder-gave yellow needles (59 mg, 57%) of **2a** (*m* = 1): m.p. 106°C, ^{1}H NMR δ 3.77 (3H, s), 5.48 (2H, br s), 6.62 (1H, dd, J = 11.0, 2.9 Hz), 6.84 (1H, d, J = 11.0 Hz), 7.12 (1H, dd, J = 12.8, 2.9 Hz), 7.20 (1H, d, J = 12.8 Hz). ^{13}C NMR δ 55.9, 113.1, 115.7, 129.6, 131.3, 152.0, 156.7, 175.4. MS (*m/z*: 70 eV) 151 (72, M$^+$), 136 (100), 123 (40). Analysis: found C 63.34, H 5.99, N 9.03; calcd for $C_8H_9NO_2$ C 63.56, H 6.00, N 9.27%.

5.4. *Preparation of 5-methoxy-2-(4-methoxybenzoylamino)tropone (1a)*

4-Methoxybenzoic acid (113 mg, 0.74 mmol) and thionyl chloride (1 cm^3) were heated at 60–70°C for 3 h. After evaporation of excess thionyl chloride, an anhydrous benzene solution of 2-amino-5-methoxytropone (56 mg, 0.37 mmol) and triethylamine (0.1 cm^3) was added to the residue and the solution heated under reflux for 6 h. The precipitates were filtered and the solvent removed under vacuum. The residue was purified by silica gel chromatography (*n*-hexane/AcOEt, 1/2). The product was washed with Na_2CO_3 solution to remove 4-methoxybenzoic acid. The resultant solid was recrystallized (*n*-hexane/AcOEt) to give yellow needles (71 mg, 67%) of **1a**. ^{1}H NMR δ 3.83 (3H, s), 3.87 (3H, s), 6.59 (1H, dd, J = 11.0, 2.6 Hz), 6.98 (2H, d, J = 8.8 Hz), 7.21 (1H, dd, J = 12.8, 2.6 Hz), 7.33 (1H, d, J = 12.8 Hz), 7.94 (2H, d, J = 8.8 Hz), 9.19 (1H, d, J = 11.0 Hz), 9.98 (1H, br s). ^{13}C NMR δ 55.4, 55.7, 110.6, 113.9 (2C), 122.2, 126.8, 129.2 (2C), 133.6, 135.8, 141.2, 161.2, 162.7, 165.6, 178.0. MS (*m/z*: 70 eV) 285 (54, M$^+$), 135 (100). Analysis: found C 67.47, H 5.41, N 4.73; calcd for $C_{16}H_{15}NO_4$ C 67.36, H 5.30, N 4.91%.

Other derivatives were prepared in a similar manner. **4a**: found C 72.42, H 6.42, N 4.64; calcd for $C_{18}H_{19}NO_3$ C 72.70, H 6.44, N 4.71%. **5a**: found C 69.25, H 6.54, N 8.91; calcd for $C_{18}H_{20}N_2O_3$ C 69.21, H 6.45, N 8.97%. **6a**: found C 54.15, H 3.20, N 4.02; calcd for $C_{16}H_{11}F_4NO_4$ C 53.79, H 3.10, N 3.92%. **7a**: found C 63.16, H 5.35, N 3.92; calcd for $C_{19}H_{19}F_2NO_4$ C 62.80, H 5.27, N 3.86%. **8a**: found C 63.16, H 5.37, N 8.13; calcd for $C_{18}H_{18}N_2O_5$ C 63.15, H 5.30, N 8.18%. **9a**: found C 70.60, H 5.64, N 8.48; calcd for $C_{19}H_{18}N_2O_3$ C 70.79, H 5.63, N 8.69%. **10c**: found C 76.34, H 8.70, N 3.31; calcd for $C_{26}H_{35}NO_3$ C 76.24, H 8.61, N 3.42%. **11a**: found C 68.24, H 5.82, N 4.26; calcd for $C_{18}H_{18}FNO_3$ C 68.56, H 5.75, N 4.44%. **12a**: found C 65.19, H 5.45, N 4.16; calcd for $C_{18}H_{18}ClNO_3$ C 65.16, H 5.47, N 4.22%. **13a**: found C 57.54, H 4.91, N 3.74; calcd for $C_{18}H_{18}BrNO_3$ C 57.46, H 4.82, N 3.72%. **14c**: ^{1}H NMR δ 0.92 (3H, t, J = 7.0 Hz), 0.98 (3H, t, J = 7.3 Hz), 1.32–1.56 (8H, m), 1.72–1.86 (4H, m), 3.96 (2H, t, J = 6.6 Hz), 4.02 (2H, t, J = 6.6 Hz), 6.89 (2H, d, J = 8.8 Hz), 6.95 (2H, d, J = 8.8 Hz), 7.50 (2H, d, J = 8.8 Hz), 7.63 (1H, br s), 7.81 (2H, d, J = 8.8 Hz). ^{13}C NMR δ 13.8, 14.0, 19.2, 22.6, 25.7, 29.1, 31.3, 31.5, 68.0, 68.2, 114.4 (2C), 114.9 (2C), 122.0 (2C), 126.9, 128.8 (2C), 131.0, 156.1, 162.0, 165.2. MS (*m/z*: 70 eV) 369 (27, M$^+$), 205 (90), 121 (100). Analysis: found C 74.50, H 8.42, N 3.56; calcd for $C_{23}H_{31}NO_3$ C 74.76, H 8.46, N 3.79%.

5.5. *X-Ray crystallographic analysis of 1h*

A pale yellow crystal of $C_{19}H_{21}NO_4$ having approximate dimensions of $0.50 \times 0.45 \times 0.30$ mm^3 was mounted on a glass fibre in a random orientation. Preliminary examination and data collection were performed with Cu K$_\alpha$ radiation (λ = 1.54184 Å) on a Nonius FR590 computer controlled kappa axis diffractometer equipped with a graphite crystal, incident beam monochromator. Cell constants and an orientation matrix for data collection were obtained from least-squares refinement, using the setting angles of 25 reflections in the range $20 < \theta < 43°$, measured by the computer controlled diagonal slit method of centring. From the systematic absences of $h\,0\,l:h = 2n$ and $0\,k\,0:k = 2n$ and from subsequent least-squares refinement, the space group was determined to be $P2_1/n$. The data were collected at a temperature of 23°C using the ω-2θ scan technique. A total of 3263 reflections were collected, of which 2940 were unique. A linear decay correction and an empirical absorption correction based on a series of psi-scans were applied to the data. The structure was solved by direct method [20] and difference Fourier syntheses. Using the 2098 reflections having intensities greater than 3.0 times their standard deviation, for 281 variable parameters, the structure was refined in full-matrix least-squares. All H atoms except N–H hydrogen were located at calculated positions and were included in the refinement with fixed isotropic thermal factors (5.0 Å^2). Atomic scattering factors were taken from *International Tables for X-ray Crystallography* [21]. The highest peak in the final difference Fourier had a height of 0.20 e Å^{-3} and the minimum negative peak had a height of -0.19 e Å^{-3}. All calculations were performed on a MicroVAX 3100 computer using MolEN [22].

5.6. *X-Ray crystallographic analysis of 7a*

A pale yellow crystal of $C_{19}H_{19}F_2NO_4$ having approximate dimensions of $0.50 \times 0.50 \times 0.20$ mm^3 was analysed. The data collection was performed with Mo K$_\alpha$ radiation (λ = 0.71069 Å) on a Rigaku RAXIS-RAPID instrument equipped with an imaging plate.

The structure was solved by direct method (*SIR92*) [23] and was refined using full-matrix least squares (*SHELXL97*) [24] based on F^2 of all independent reflections measured.

References

[1] DEMUS, D., 1998, *Handbook of Liquid Crystals*, Vol. 1, edited by D. Demus, J. Goodby, G. W. Gray, H.-W. Spiess, and V. Vill (Weinheim: Wiley-VCH).

[2] MORI, A., YOKOO, M., HASHIMOTO, M., UJIIE, S., DIELE, S., BAUMEISTER, U., and TSCHIERSKE, C., 2003, *J. Am. chem. Soc.*, **125,** 6620.

[3] HASHIMOTO, M., UJIIE, S., and MORI, A., 2000, *Chem. Lett.*, 758.

[4] MORI, A., KATO, N., TAKESHITA, H., NIMURA, R., ISOBE, M., JIN, C., and UJIIE, S., 2001, *Liq. Cryst.*, **28,** 1425.

[5] MORI, A., KATAHIRA, K., KIDA, K., and TAKESHITA, H., 1992, *Chem. Lett.*, 1767.

[6] MORI, A., HIRAYAMA, K., KATO, N., TAKESHITA, H., and UJIIE, S., 1997, *Chem. Lett.*, 509.

[7] MORI, A., UCHIDA, M., and TAKESHITA, H., 1989, *Chem. Lett.*, 591; MORI, A., TAKESHITA, H., KIDA, K., and UCHIDA, M., 1990, *J. Am. chem. Soc.*, **112,** 8635; KIDA, K., MORI, A., and TAKESHITA, H., 1991, *Mol. Cryst. liq. Cryst.*, **199,** 387.

[8] BELMER, J., PARRA, M., ZUNIGA, C., FUENTES, G., MARCOS, M., and SERRANO, J. L., 1999, *Liq. Cryst.*, **26,** 9.

[9] HASHIMOTO, M., UJIIE, S., and MORI, A., 2003, *Adv. Mater.*, **15,** 797.

[10] NISHIO, M., HIROTA, M., and UMEZAWA, Y., 1989, *The CH/π Interaction. Evidence, Nature, and Consequences* (New York: Wiley-VCH); TAKAHASHI, O., KOHNO, Y., IWASAKI, S., IWAOKA, M., TOMODA, S., UMEZAWA, Y., TSUBOYAMA, S., and NISHIO, M., 2001, *Bull. chem. Soc., Jpn.*, **74,** 2421.

[11] MIYAMURA, K., MIHARA, A., FUJII, T., GOHSHI, Y., and ISHII, Y., 1995, *J. Am. chem. Soc.*, **117,** 2377.

[12] WEN, J., XU, Y., TIAN, M., and CHAN, Q., 1993, *Ferroelectrics*, **148,** 129.

[13] BEGUIN, A., DUBOIS, J. C., and ZANN, A., 1978, *Eur. Pat. Appl.*, EP 11.002.

[14] COATES, D., 1987, *Liq. Cryst.*, **2,** 63; CHIENG, Y. H., AMES, A. E., GOUDIANA, R. A., and ADAMS, T. G., 1991, *Mol. Cryst. liq. Cryst.*, **208,** 85.

[15] COATES, D., and GRAY, G. W., 1975, *Mol. Cryst. liq. Cryst.*, **31,** 275.

[16] GAHREN, A., 1908, PhD thesis, Halle University, Germany.

[17] VILL, V. *LiqCryst 4.3-Database of Liquid Crystalline Compounds*, Fujitsu Kyushu Engineering, Fukuoka, Japan.

[18] GRAY, G. W., 1979, *The Molecular Physics of Liquid Crystals*, edited by G. R. Luckhurst and G. W. Gray (Academic Press), p 1.

[19] NOZOE, T., SETO, S., ITO, S., SATO, M., and KATONO, T., 1952, *Proc. Japan Acad.*, **28,** 488.

[20] MAIN, P., FISKE, S. J., HULL, S. E., LESSINGER, L., GERMAIN, G., DECLERCQ, J.-P., and WOOLFSON, M. M., 1982, *MULTAN11/82*, A System of Computer Programs for the Automatic Solution of Crystal Structures from X-ray Diffraction Data, University of York, England, and Louvain, Belgium.

[21] CROMER, D. T., and WABER, J. T., 1974, *International Tables for X-ray Crystallography*, Vol. IV, (Birmingham; Kynoch Press), Table 2.2A.

[22] FAIR, C. K., 1990, *MolEN, An Interactive Intelligent System for Crystal Structure Analysis*, Enraf-Nonius, Delft, The Netherlands.

[23] ALTOMARE, M. C., BURLA, M., CAMALLI, G., CASCARANO, C., GIACOVAZZO, A., GUAGLIARDI, G., and POLIDORI, J., 1994, *J. appl. Cryst.*, **27,** 435.

[24] SHELDRICK, G. M., 1997, *SHELXL97, Program for the Refinement of Crystal Structures*, University of Göttingen, Germany.